Available online at www.sciencedirect.com
SCIENCE DIRECT
Journal of Sound and Vibration 295 (2006) 810–826
JOURNAL OF SOUND AND VIBRATION
www.elsevier.com/locate/jsvi

Investigation on improved Gabor order tracking technique and its applications

Min-Chun Pan*, Chun-Ching Chiu

Department of Mechanical Engineering, National Central University, No. 300, Jhongda Road, Jhongli City, Taoyuan County 320, Taiwan, ROC

Received 25 November 2004; received in revised form 10 January 2006; accepted 24 January 2006
Available online 11 April 2006

Abstract

The study proposes an improved Gabor order tracking (GOT) technique to cope with crossing-order/spectral components that cannot be effectively separated by using the original GOT scheme. The improvement aids both the reconstruction and interpretation of two crossing orders/spectra such as a transmission-element-regarding order and a structural resonance. The dual function of the Gabor elementary function can affect the precision of tracked orders. In the paper, its influence on the computed Gabor expansion coefficients is investigated. For applying the improved scheme in practical works, the separation and extraction of close-order components of vibration signals measured from a transmission-element test bench is illustrated by using both the GOT and Vold–Kalman filtering OT methods. Additionally, comparisons between these two schemes are summarized from processing results. The other experimental work demonstrates the ranking of noise components from a riding electric scooter. Singled-out dominant noise sources can be referred for subsequent design-remodeling tasks.

1. Introduction

Mechanical systems under periodic loading due to rotating operation usually respond in measurements with a superposition of sine waves whose frequencies are integer (or fractional) multiples of the reference shaft speed. The fundamental frequency corresponding to the shaft speed is called a basic order. The order tracking (OT) techniques have been applied in the analysis of dynamic signals measured from rotary machinery for more than two decades. The need for the OT techniques is evident in the investigation of rotary machinery, such as performing electrical-machine (motor and generator) acceptance tests and examining noise-level of vehicles. Additionally, spectral (or order) components contributing to the noise-vibration-and-harshness (NVH) concerns can be identified effectively by using these OT approaches [1–3].

All developed OT techniques can be classified into two categories, i.e., waveform *reconstruction* and *non-reconstruction* schemes. The waveform *non-reconstruction* schemes, which can process signals to be

*Corresponding author. Tel.: +886 3 4267312; fax: +886 3 4254501.
E-mail address: pan_minc@cc.ncu.edu.tw (M.-C. Pan).

0022-460X/$ - see front matter © 2006 Elsevier Ltd. All rights reserved.
doi:10.1016/j.jsv.2006.01.046

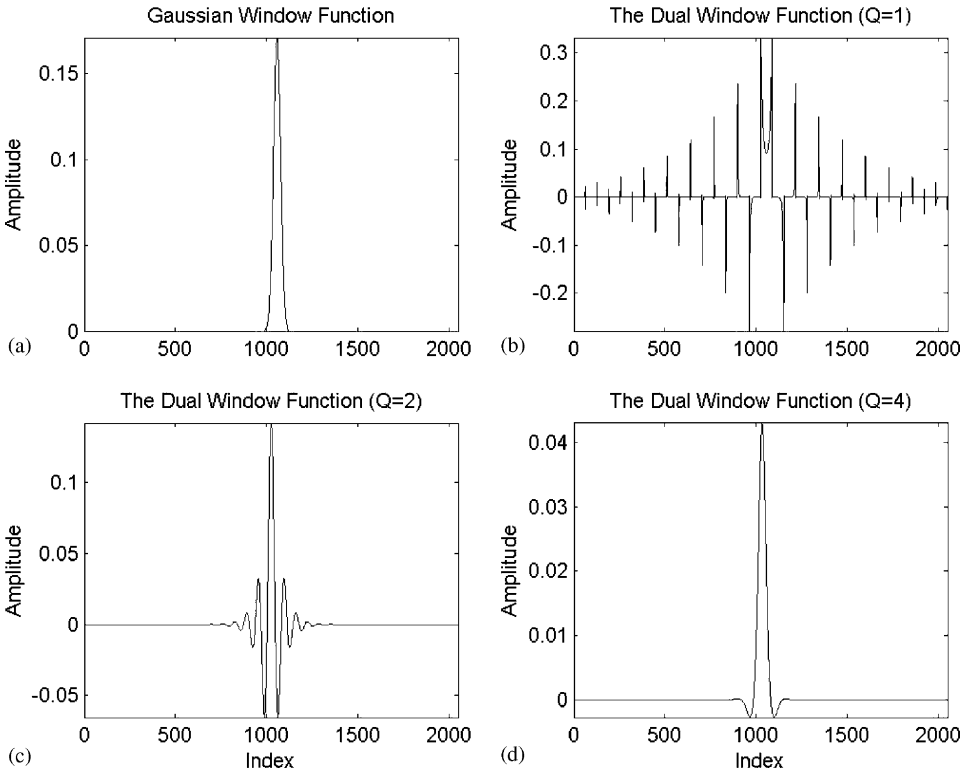

Fig. 1. Gabor dual function with various over-sampling rate: (a) Gaussian window as a Gabor elementary function; dual function with (b) $Q = 1$, (c) $Q = 2$, and (d) $Q = 4$.

characterized into a rev/min-frequency (rev/minF) or rev/min-order plane but not reconstruct the waveforms of specific orders, include the short-time Fourier transform (STFT) based order analysis, and the resampling scheme [1,3]. In contrast, the waveform *reconstruction* schemes, which enable to extract specific spectral/order components and reconstruct their time histories, include the angular-velocity/angular-displacement Vold–Kalman filtering (VKF) OT [4–6], and Gabor order tracking (GOT) [2,7] approaches, etc. It should be noted that although the GOT scheme is applied to reconstruct order components mainly, the simultaneous time–frequency (or rev/min–frequency) illustration of the computed signal's Gabor coefficients can also characterize orders of interest in a two-dimensional plane. Comparing the GOT with other OT schemes such as the resampling and VKF_OT methods, etc., only the GOT technique links two families of signal processing tools together, i.e., the time–frequency representation (TFR) that handles transient and nonstationary signals, and the order tracking techniques that characterize and reconstruct the order/spectral components of interest embedded in a processed signal. Moreover, it is rather straightforward to use the GOT technique that associates with flexible tracking-mask selection to extract and reconstruct spectral components. The information of shaft speed can even be missing while the GOT is applied for rotary machines. For some applications, the GOT scheme can be employed in singling out and reconstructing the waveforms of target spectral components without losing tiny information from transient or nonstationary signals, such as seismic and biomedical signals [8], etc. The GOT technique was proposed with extremely good selectivity on the extracted signal component [7]. But in the finite width of tracking masks, all spectral artifacts from smearing errors and other unwanted components may also be captured to reproduce the time histories. This makes the decoupling and separation of cross and close orders impossible. The drawback affects its application especially in the extraction and interpretation of components crossing with other signatures. So far the issue has not drawn researchers' attention yet.

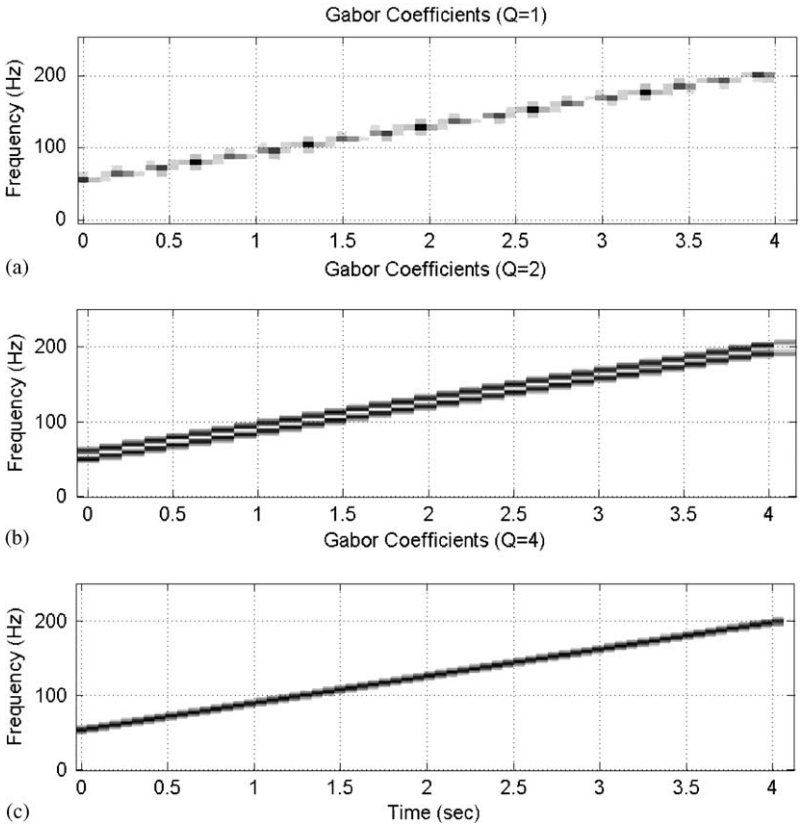

Fig. 2. TFR illustration of Gabor coefficients: (a) $Q = 1$, (b) $Q = 2$, and (c) $Q = 4$.

Fortunately, spectral or order components to be tracked generally vary in amplitude steadily due to mechanical inertia, and seldom fluctuate with an impact form normally. To tackle the crossing-order/spectral problem, in the study, an improved algorithm is proposed by using both image edge-detection and averaging computation, which corresponds to the afore-mentioned engineering phenomena. Synthetic signals are designed and applied to evaluate the developed schemes. The characteristic features of the technique to separate close orders and decouple crossing spectral components are highlighted. Some practical works are conducted for validation including (1) the separation of close orders of vibration signals measured from a transmission-element test bench, and (2) the ranking of riding noise emitted from an electric scooter. Comparisons are briefed between the proposed technique and VKF_OT approaches.

2. Theoretical basis

The Gabor transform can process and transfer a signal to obtain its Gabor expansion coefficients that can be characterized in a TF plane. Additionally, the Gabor expansion function like the Fourier series can be employed to reconstruct the waveform of the original signal with the Gabor expansion coefficients computed previously [9,10]. Furthermore, Qian and Albright [2,7] exploited the Gabor transform/expansion to track a specific order/spectral component, or a combination of orders. The procedure to extract selected orders is called the GOT. The need to improve waveform reconstruction at the occurrence of order/spectral crossing is, however, nontrivial due to the deficiency of computation algorithm. The section addresses the basic principle and numerical implementation of the *improved* GOT scheme.

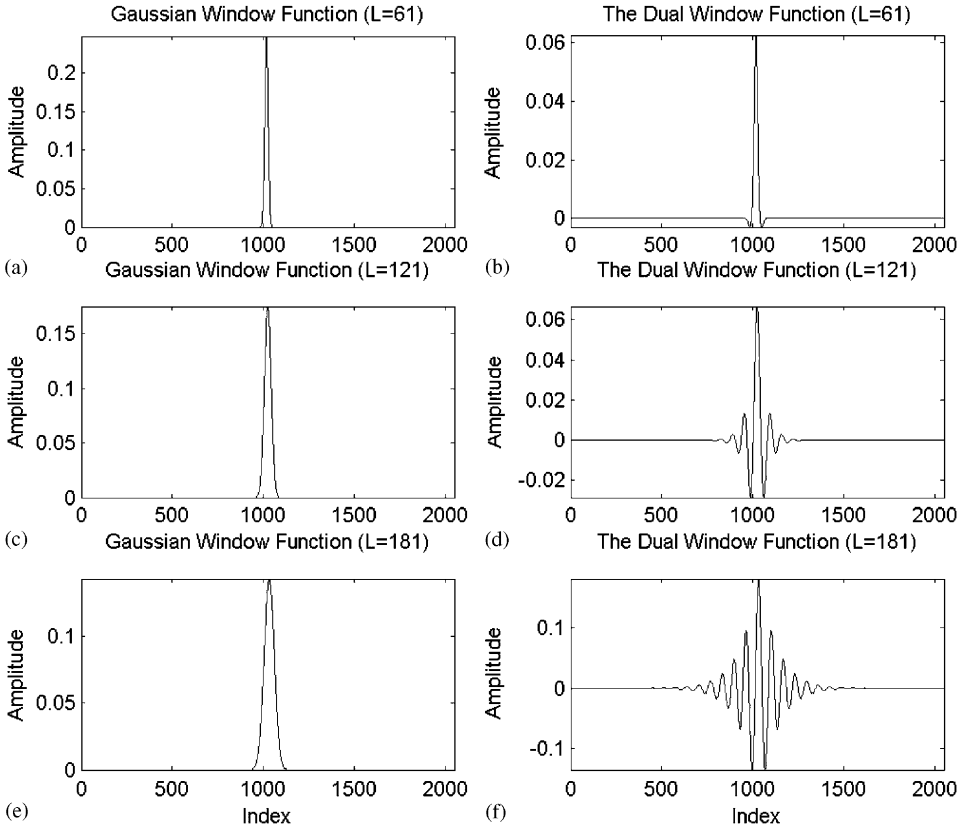

Fig. 3. Gaussian Gabor elementary functions (a), (c), and (e) and corresponding dual functions (b), (d), and (f) with various lengths, $L = 61$, 121, 181, respectively.

2.1. Gabor expansion and transform

Gabor [9] proposed a signal expansion using both shift and modulated Gabor elementary functions. That is, the Gabor expansion of a signal $\phi(t)$ to be processed can be expressed by

$$\phi(t) = \sum_{m=-\infty}^{\infty} \sum_{n=-\infty}^{\infty} a_{m,n}\, g_{m,n}(t), \tag{1}$$

where $a_{m,n}$ denote the Gabor expansion coefficients, and $g_{m,n}(t)$ the shift and modulated forms of the Gabor elementary function, $g(t)$. The Gabor expansion coefficients can further be characterized to illustrate the signal's time and frequency features in a TF plane. Eq. (1) means the shift and modulated Gabor elementary functions,

$$g_{m,n}(t) = g(t - mT)\, \mathrm{e}^{\mathrm{j}n\Omega t}, \quad m, n = 0, \pm 1, \pm 2, \pm 3, \ldots, \tag{2}$$

as basic functions can compose any signals, where T (s) and Ω (rad/s) are the time and frequency periods, respectively, of the Gabor expansion coefficients. For evaluating the Gabor expansion coefficients, $a_{m,n}$, Bastiaans [10,11] proposed using the Gabor transform (or called *sampled* STFT), i.e.,

$$a_{m,n} = \int_{-\infty}^{\infty} \phi(t)\, \gamma_{m,n}^{*}(t)\, \mathrm{d}t = \mathrm{STFT}(mT, n\Omega), \quad m, n = 0, \pm 1, \pm 2, \pm 3, \ldots, \tag{3}$$

where $\gamma_{m,n}(t) = \gamma(t - mT)\mathrm{e}^{\mathrm{j}n\Omega t}$ are the shift and modulated forms of a corresponding dual function of the elementary function, and * denotes a complex conjugate. For the Gabor expansion coefficients illustrated in a simultaneous TF plane, it requires critical sampling ($T\Omega = 2\pi$) or over sampling ($T\Omega < 2\pi$) for completely

reconstructing a signal. For a perfect reconstruction, $g(t)$ and $\gamma(t)$ are biorthogonal functions each other. Thus the reconstruction equation, Eq. (1), can also be expressed by [10,11]

$$\phi(t) = \sum_{m=-\infty}^{\infty} \sum_{n=-\infty}^{\infty} a_{m,n}\, \gamma(t - mT)\, \mathrm{e}^{\mathrm{j}n\Omega t} \equiv \sum_{m=-\infty}^{\infty} \sum_{n=-\infty}^{\infty} a_{m,n}\, \gamma_{m,n}(t), \tag{4}$$

where $a_{m,n} = \int_{-\infty}^{\infty} \phi(t)\, g^*(t - mT)\, \mathrm{e}^{-\mathrm{j}n\Omega t}\, \mathrm{d}t = \int_{-\infty}^{\infty} \phi(t)\, g^*_{m,n}(t)\, \mathrm{d}t$. Obviously, $\gamma_{m,n}(t)$ are the corresponding dual function of $g_{m,n}(t)$. The applicable values of shift and modulated Gabor elementary functions make the TF localization for a reconstructed signal from the Gabor expansion. In the selection of a Gabor elementary function, the Gaussian function is usually first considered due to its minimum TF resolution multiplication. Some useful technical papers can be referred for the implementation of numerical details such as the evaluation of Gabor transform [12–14]. It is worth mentioning that the Gabor expansion associated with Gabor transform basically differs from the window Fourier transform (WFT), sometimes called STFT. The evaluation of WFT of a signal is to move a selected weighting function (or window) along the signal to be processed [3]. The computed WFT can characterize and illustrate the features of the signal in a TF plane. But, the handled signal cannot be reconstructed through the used WFT as no biorthogonal relationship for the used window functions is required, and no inverse transform exists while using the WFT. Conversely, the Gabor expansion associated with Gabor coefficients and corresponding elementary functions enables to fully reconstruct the processed signal. As results, while the Gabor coefficients characterized in an rev/minF (or rev/min-order) plane are partially selected, the waveform of an embedded single or multiple order/spectral components can be reconstructed. This is the basic idea of the GOT technique that cannot be accomplished through the WFT (or STFT).

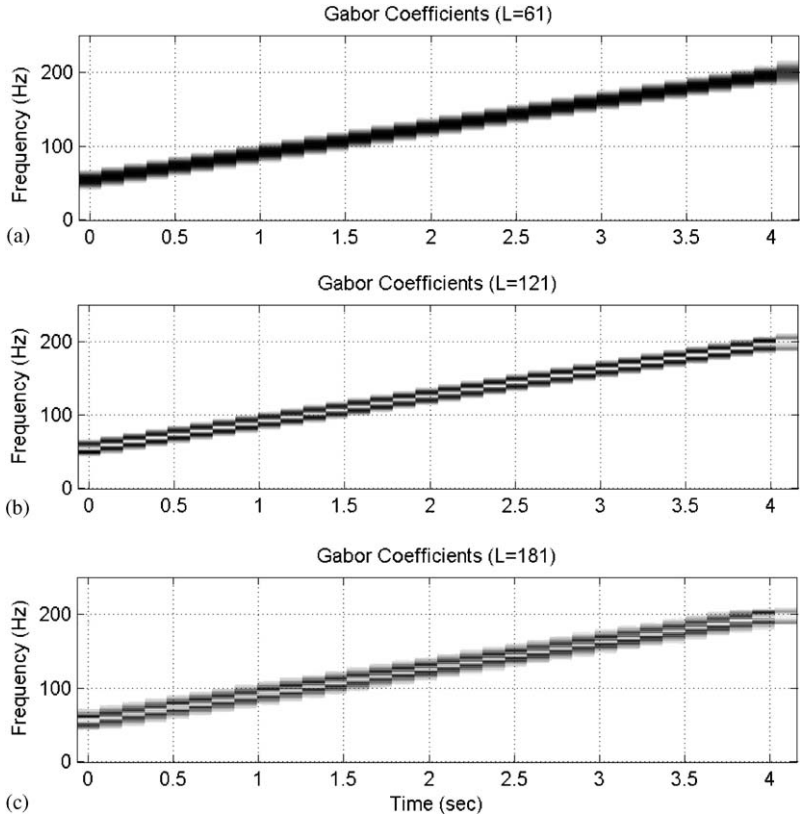

Fig. 4. TFR illustration of Gabor coefficients with various lengths: (a) $L = 61$, (b) $L = 121$, and (c) $L = 181$.

2.2. Influences of dual functions on Gabor expansions

The subsection discusses the influences of the over-sampling rates (Q), and the length (L) of the elementary function on the Gabor expansion coefficients. The over-sampling rate can be defined by

$$\text{oversampling rate } (Q) = \frac{\text{numbers of signal sample } (L)}{\text{product of sampling step } (T\Omega)}, \tag{5}$$

where $Q = 1$ is called critical sampling, and $Q > 1$ over-sampling. For a reliable waveform reconstruction, the over-sampling rate must satisfy $Q \geqslant 1$. As an example, for the length of a Gaussian elementary function with 127 points, the computed dual functions with over-sampling rates $Q = 1$, 2, and 4, respectively, are illustrated in Fig. 1. The TFR illustration of corresponding Gabor expansion coefficients of a linear

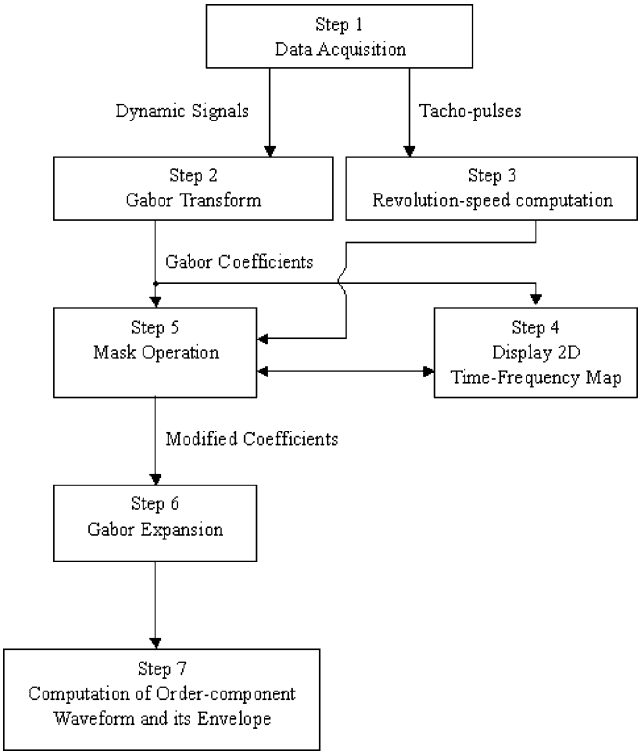

Fig. 5. Flow diagram to complete an improved GOT procedure.

Table 1
Synthetic signal and its order/spectral components

Synthetic signal to be analyzed				
Order components				
Order	1	6	8	18
Amplitude (linearly increasing)	0–10	0–13	0–15	0–8
Resonance				
Frequency (Hz)	700			
Amplitude	10			
Background noise				
Maximum amplitude	3			

frequency-modulation signal $x(t)$ equated with

$$x(t) = \sin\left[2\pi\left(60t + 17.5t^2\right)\right] \tag{6}$$

is shown in Fig. 2. The signal with an instant frequency $(60 + 35t)$ Hz actually indicates at the time $t = 0$ and 4 s with frequencies of 60 and 200 Hz, respectively. It is noted that as the computed dual function with a higher Q more resembles the elementary function, the evaluated Gabor expansion coefficients can characterize TF features of the reconstructed signal better. For the influences of elementary-function length on Gabor expansion coefficients, Fig. 3 illustrates the Gaussian Gabor elementary functions with different lengths of 61, 121, 181, respectively, and their corresponding dual functions with the same over-sampling rate $Q = 4$. Fig. 4 shows the computed Gabor expansion coefficients that are characterized in a TF plane. Some remarks can be concluded as follows, which are used as guidelines for subsequent validation work. As evaluating the Gabor expansion coefficients of a dynamic signal, one can tune both the elementary-function length and over-sampling rate to make the dual function as identical to the Gabor function as possible. The dual function more resembling a Gaussian function can result in better TF localization of computed Gabor expansion coefficients. For instance, in the case of Fig. 3, while using $L = 61$ as the length of Gaussian elementary function, it is satisfied to choose the over-sampling rate $Q = 4$ for obtaining the dual function. While $L = 121$ is employed, the chosen Q, however, needs to be even larger than 4. It should be noted that although shorter elementary function yielding smaller over-sampling rate can have better computation efficiency, it causes a worse frequency resolution that affects effective separation of multiple-order/spectral components. It is shown that for the GOT there exist tradeoffs between the length of elementary function, over-sampling rate, computation efficiency, and TF resolution while used in tracking target spectral/order components.

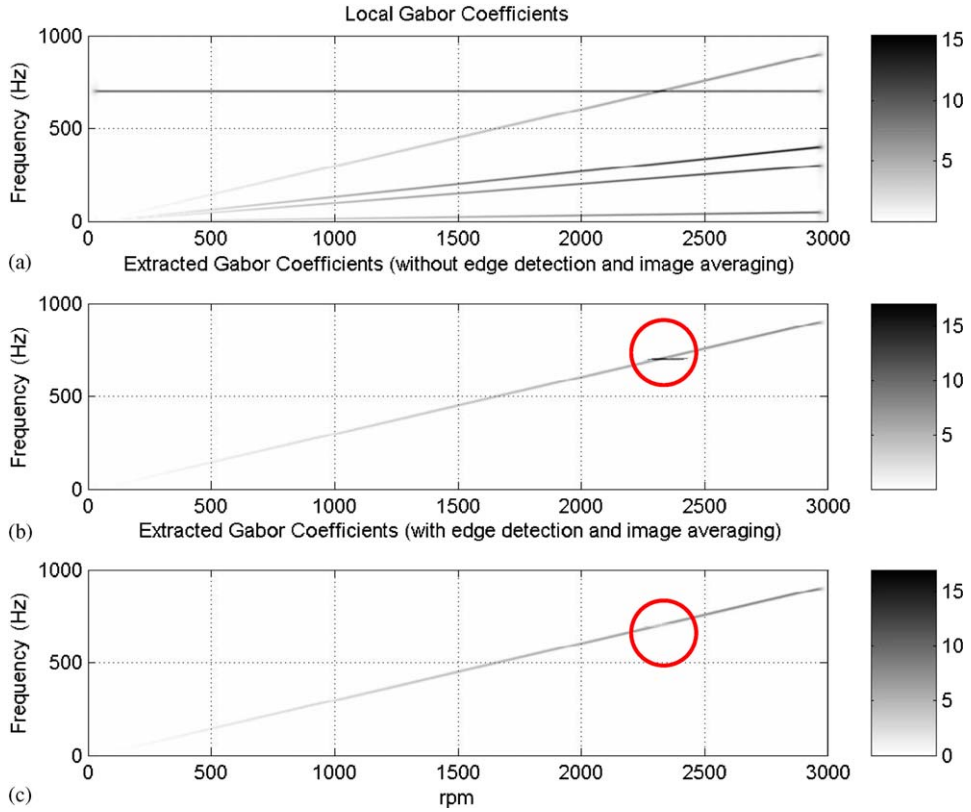

Fig. 6. Rev/minF charts of Gabor coefficients of the synthetic signal and tracked order-18 component: (a) synthetic signal, (b) extracted original order-18 after using a mask on plot (a), (c) extracted improved order-18 using the modified scheme. The circles on plots (b) and (c) indicate order/spectral-crossing occurrences.

2.3. Improved GOT scheme

For the Gabor order tracking to extract specific order/spectral components, first proposed by Albright and Qian [7], only the Gabor coefficients of those target signatures are employed in the Gabor expansion function and computed for their time histories. To obtain the target Gabor coefficients, the characterized rev/minF (or TF) map of overall Gabor coefficients are multiplied by a designated mask with a value of 1. Crossing order/spectral components cannot be effectively decoupled while their waveforms are reconstructed by simply setting

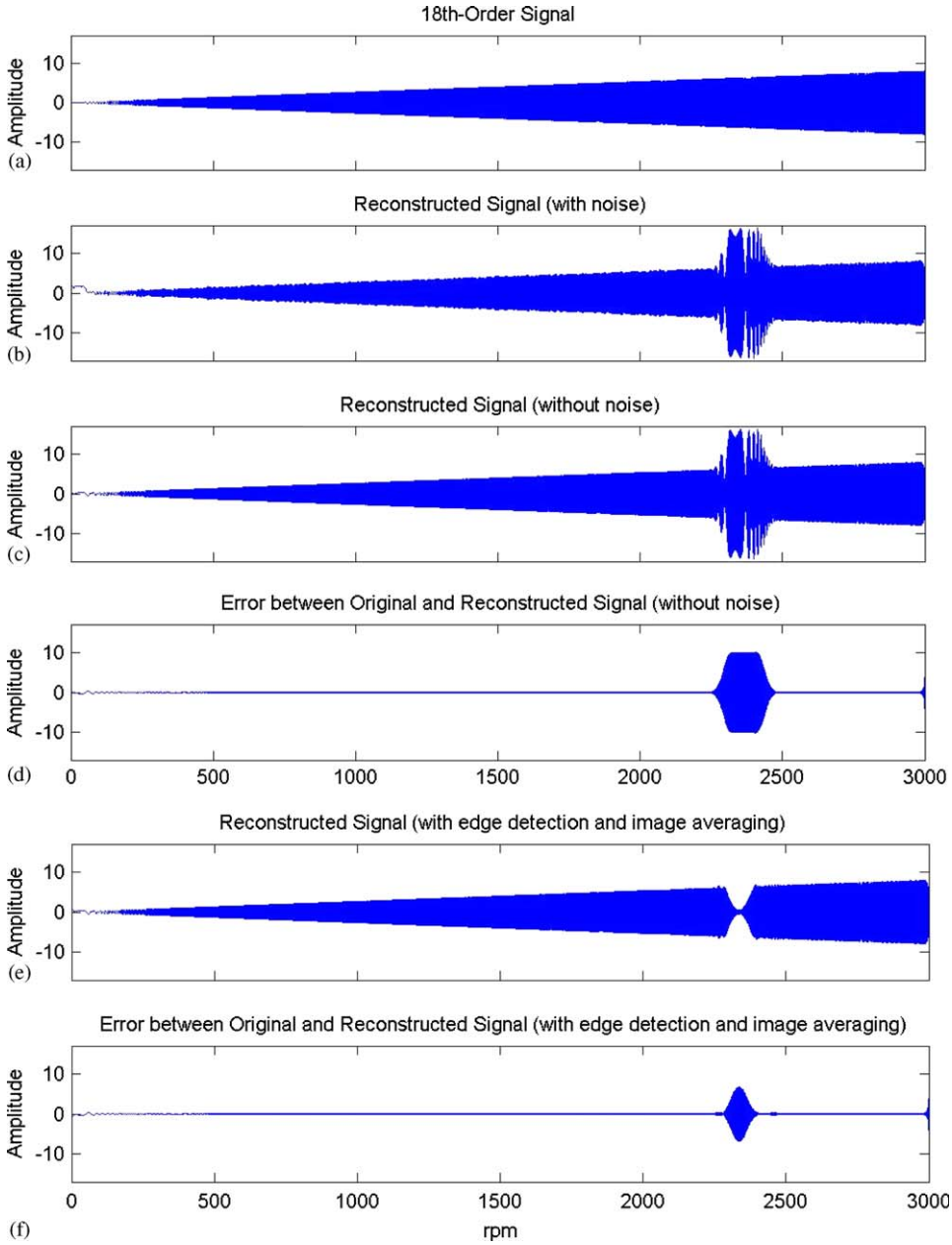

Fig. 7. Illustration of (extracted) order-18 component: (a) synthesized order-18 waveform, (b) extracted order-18 waveform, (c) reconstructed order-18 waveform from noise-free signal, (d) errors between exact and estimated (original scheme), (e) extracted order-18 waveform with improved scheme, and (f) errors between exact and estimated (improved scheme).

masks on the rev/minF map of Gabor expansion coefficients. It is an inherent consequence that the waveform of all significant and tiny signatures under the masks will be recovered. To complete an improved GOT procedure is demonstrated in the flow diagram of Fig. 5 and summarized below.

- After evaluating and characterizing the Gabor expansion coefficients (Step 2) in an rev/minF (or TF) plane (Step 4), one can prepare an rev/minF (or TF) mask with a specific width of pixels, which covers target order/spectral components (mono-components or multi-components) of interest.
- The Gabor expansion coefficients are multiplied by a designated mask (Step 5) to obtain the Gabor coefficients of target order components. It should be noted that other artifacts under the mask, especially for those crossing with the target order, are also included.
- To get rid of the contribution of unwanted components to the reconstructed waveforms, modified coefficients for those order/spectral crossing occurrences are computed sequentially through edge detection and removing of crossing regions, and image averaging. In the study, the Canny method is applied as the image edge detector that is optimal for step edges corrupted by white noise [15]. The Canny method finds edges by looking for local maxima of the gradient of image I, here the characterized Gabor coefficients. The gradient is calculated using the derivative ($G_{\boldsymbol{n}}$) of a Gaussian filter, $G(x, y)$,

$$G(x,y) = \frac{1}{\sqrt{2\pi}\sigma}\, \mathrm{e}^{(-x^2+y^2)/2\sigma^2}, \tag{7}$$

where σ is a standard deviation of the associated probability distribution, and $G_{\boldsymbol{n}} = \frac{\partial G}{\partial \boldsymbol{n}} = \mathbf{n} \cdot \nabla G$. It can be shown that convolving the image I with an operator $G_{\boldsymbol{n}}$ forms a simple and effective directional operation. The edge location is then at the local maximum of the image I convolved with the operator $G_{\boldsymbol{n}}$ in the direction $\mathbf{n}$. That is

$$\frac{\partial}{\partial \mathbf{n}}\, G_{\boldsymbol{n}} * I = 0 \tag{8}$$

or equivalently

$$\frac{\partial^2}{\partial \mathbf{n}^2}\, G * I = 0, \tag{9}$$

where $*$ denotes convolution. Then, the crossing regions are removed while the edges are detected. Basically, the energy levels (now in a format of Gabor-coefficient image) of any signal components arising from the operation of rotary machinery seldom change abruptly due to the inertia of rotating elements.

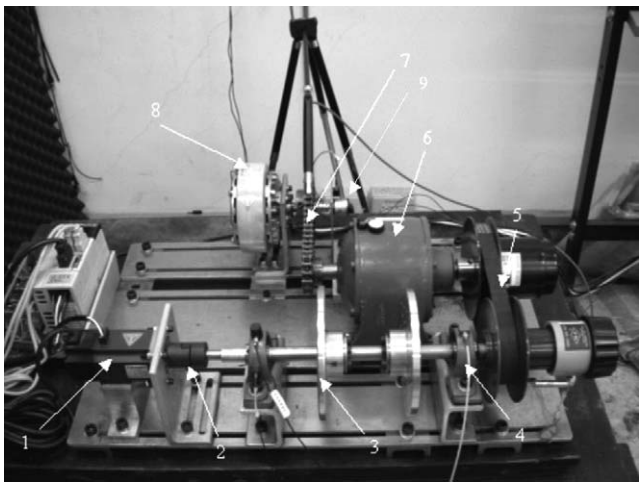

Fig. 8. Transmission-element test bench: 1, servo-motor; 2, flexible coupling; 3, rotors; 4, bearings; 5, cogged V-belt; 6, gear box; 7, roller chain and 8, electric–magnetic brake.

A steady transition of amplitudes from low to high speed (or high to low speed) exists in general situations. The modified Gabor coefficients of the removed regions are obtained by averaging the Gabor-coefficients data near the crossing regions. Thus the processing step after Step 5 (mask operation) can be improved to obtain modified Gabor expansion coefficients.

- Finally, the Gabor expansion equation (4) is used to reconstruct the waveforms of target order/spectral components (Step 6 and 7) through the modified Gabor coefficients.

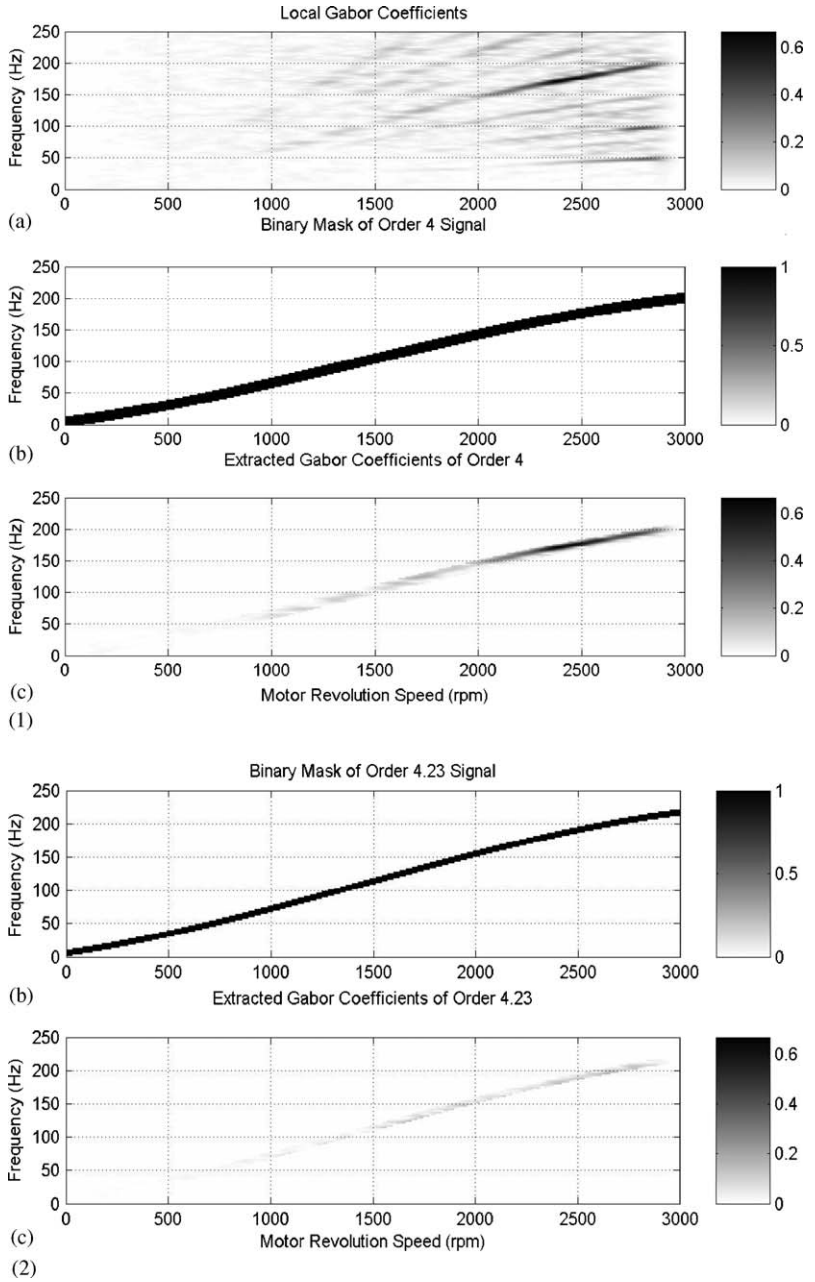

Fig. 9. Extraction of the order-4 and order-4.23 components: (1)(a) (partial) rev/minF plot of Gabor coefficients, (1)(b) TF mask on order-4 component, (1)(c) masked Gabor coefficients of order-4 and (2)(b) TF mask on order-4.23 component, (2)(c) masked Gabor coefficients of order-4.23.

Based on these Gabor expansion OT processes, to reconstruct order components of interest is quite straightforward and comprehensible. Additionally, as the technique is applied in reconstructing the waveforms of order components in signals measured from rotary machinery, it is still acceptable and feasible for shaft speed of absence. To justify its performance, a set of synthetic signal with four order components and one resonance associated with noise, as shown in Table 1, is designated. Fig. 6(a) charts the rev/minF plot of computed Gabor expansion coefficients, and Figs. 6(b) and (c) illustrate original masked coefficients and modified ones of order-18 component, respectively, by using the original and improved schemes. All those masked coefficients (Figs. 6(b) and (c)) are employed in the next waveform-reconstruction procedure. It is found that the original GOT scheme cannot get rid of 700 Hz resonance near 2350 rev/min, but improved scheme can obtain much better results. Circles in Fig. 6 indicate order/spectral crossing occurrences. By substituting those computed coefficients into the Gabor expansion function, Eq. (1), one can obtain the waveforms of the order-18 component. Fig. 7 demonstrates the errors between the designated and reconstructed waveforms using original and improved schemes, respectively. It is noted that less errors can be achieved using the proposed method although it is still not perfect. As the modified Gabor coefficients at order/spectral crossing occurrences are computed by averaging the Gabor coefficients outside crossing region, the modified coefficients may result in the reconstructed waveform a two-side concave shape.

3. Engineering applications

In the section, the proposed technique is applied in practical works, such as (1) decoupling close dynamic signatures measured from a transmission-element test bench and (2) ranking noise components arising from different machine elements.

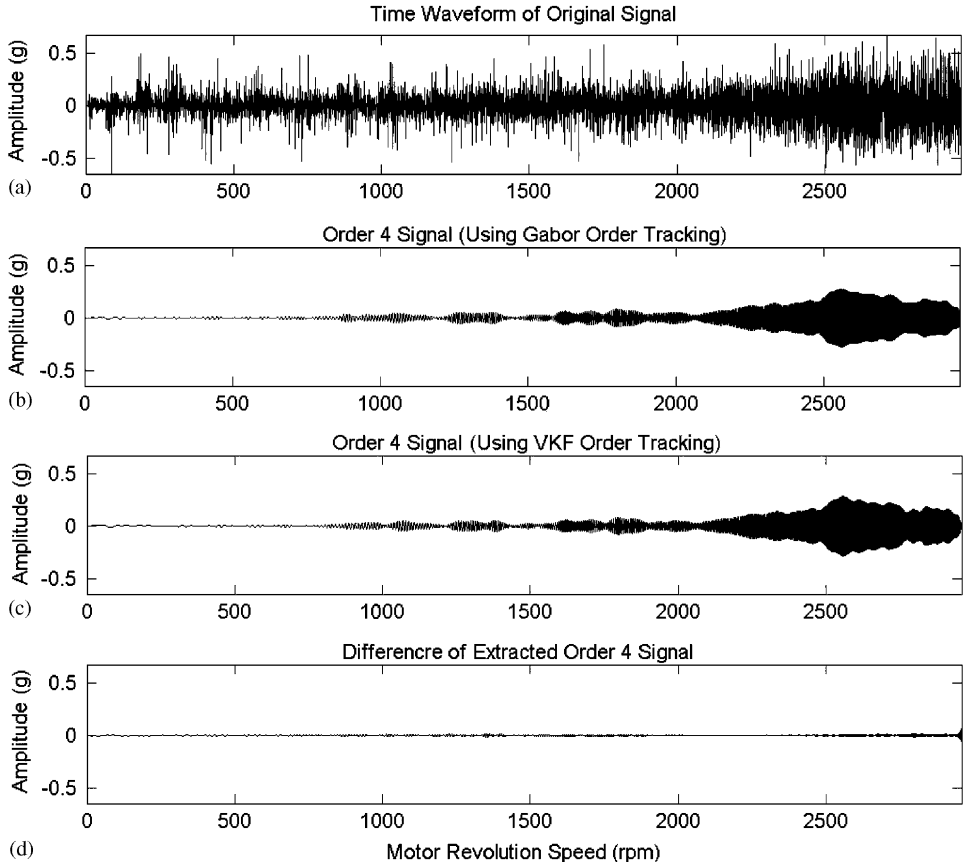

Fig. 10. Extraction of the order-4 waveform: (a) measured time waveform, (b) reconstructed by the GOT, (c) reconstructed by the VKF_OT, and (d) waveform difference between (b) and (c).

3.1. Close-order decoupling for transmission-component test bench

The improved GOT scheme is now applied in decoupling close orders emitted from transmission components of an in-house test bench, and investigating dynamic characteristics of the system as well. Machine parts include a servomotor as the power source, a multiple-component transmission system

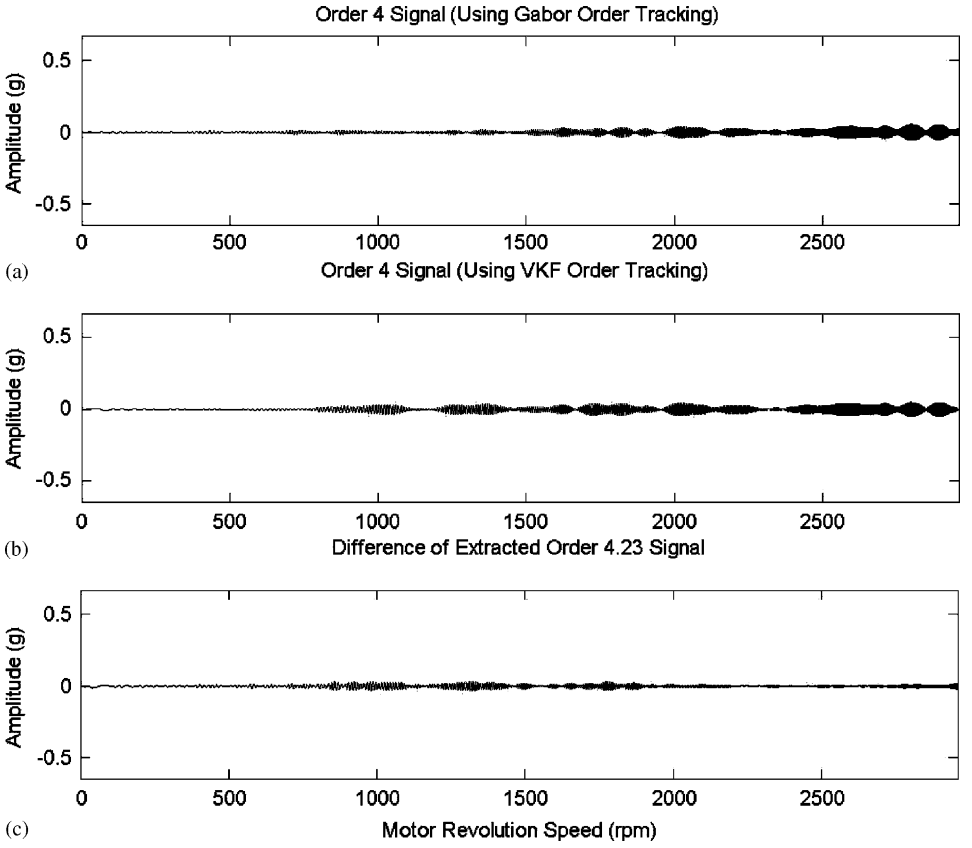

Fig. 11. Extraction of the order-4.23 waveform: (a) reconstructed by the GOT, (b) reconstructed by the VKF_OT, and (c) waveform difference between (a) and (b).

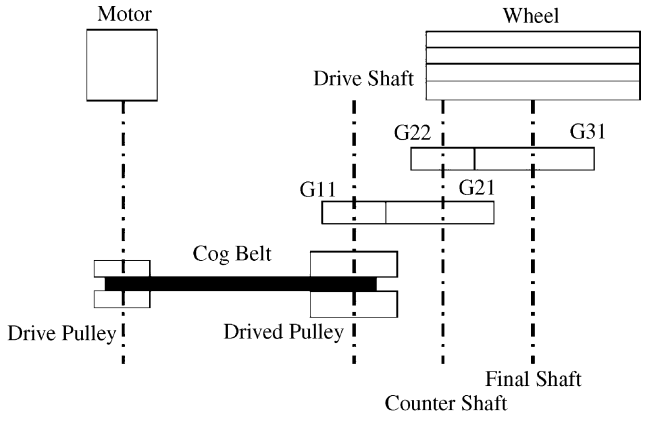

Fig. 12. Schematic of transmission system of test electric scooter.

consisting of a tunable-speed-ratio belt-driven set, a two-stage speed-reduction gearbox with a speed ratio of 5, and a roller-chain set with a speed ratio of 12/7. Additionally, an electro-magnetic brake is employed to serve as the load of the system. The test bench includes a flywheel set with two rotors for simulating different imbalancing conditions. Fig. 8 illustrates the test bench and measurement setup. Since an Odem flexible coupling (item 2 in Fig. 8) is used to transmit power, vibration signatures of the order-4 components corresponding to motor speed are dominant during operation [16]. The speed-ratio of the belt-driven set is tuned to give the meshing frequency of the second gear pair an order of 4.23. Thus close vibration order components are synthesized. In this case, the vibration level of order-4 component are as around five multiple as that of order-4.23.

Both order-4 and order-4.23 rev/minF masks (Figs. 9(1)(b) and (2)(b)) are first computed according to the motor sped, and then the Gabor expansion coefficients of these two order components are extracted, as shown in Figs. 9(1)(c) and (2)(c). Reconstructed order-4 waveform (Fig. 10(b)) is computed through Gabor expansion function. The result is compared with that (Fig. 10(c)) using the VKF_OT technique as a benchmark, as it is well noted that the VKF_OT scheme through the least square computation is somewhat a standardized waveform-reconstruction OT technique. It is found the difference of reconstructed waveforms obtained by these two schemes is quite limited, as shown in Fig. 10(d). Likewise, the time-history of order-4.23 component can be extracted and reconstructed with the same procedure. Fig. 11 illustrates the waveforms and their difference through two schemes. This procedure demonstrates that close components can be separated effectively using the improved GOT. One significant feature for the GOT scheme superior to the VKF_OT is without end effects on the reconstructed waveform.

3.2. Riding-noise ranking for electric scooter

For the NVH concerns of rotary machinery, it is nontrivial for design remodeling to single out critical machine components that dominate vibration and noise emission. The second validation task is to rank riding noise for electric scooters. The test scooter is driven by a brushless DC motor, and its mechanical power is transmitted through continuous variable transmission (CVT) mechanism associated with two stages of speed

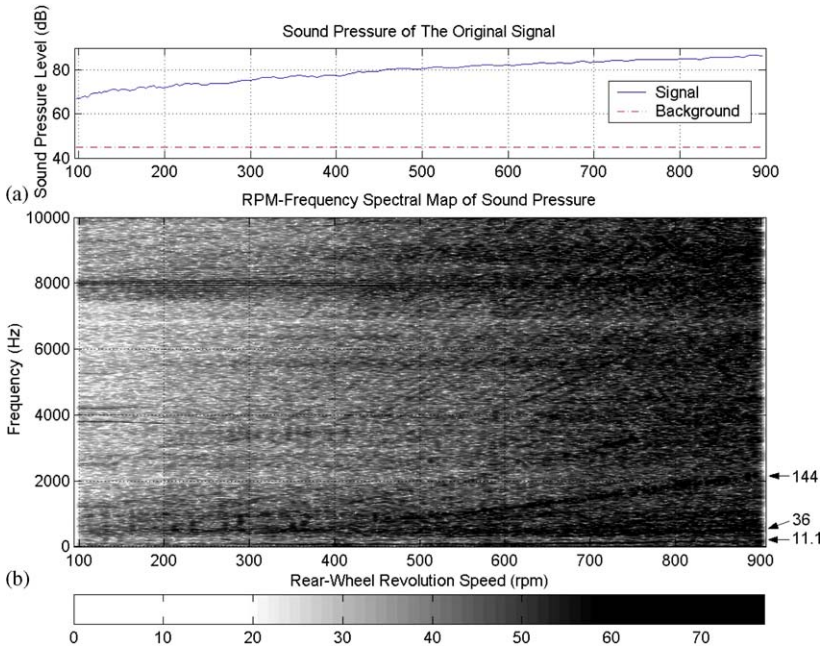

Fig. 13. Noise measurement on test electric scooter: (a) sound pressure level along rear wheel speed and (b) rev/min spectrum of Gabor expansion coefficients indicated with characteristic orders.

reduction gears, i.e., helical and spur gears. The rotating parts of the CVT system include a speed-varying cog belt and two CVT sheaves, where a forming cooling centrifugal fan attached to the driving sheave. Fig. 12 illustrates the schematic of its transmission system. For each riding-noise measurement, total acquiring time is around 8.3 s. The scooter steadily speeds up from 100 rev/min of rear-wheel speed to a high speed of 900 rev/min. Both motor and rear-wheel speeds are evaluated through measured tacho-pulses. Two channels of riding noise are acquired using precision microphones with a sampling frequency of 20 kHz, and the low-pass anti-aliasing set at 10 kHz.

We can outline potential featured orders in riding noise probably emitted from the transmission system, as summarized in Ref. [3]. In the case, orders based upon rear-wheel (or engine) speed are not crossing surely, but some transmission orders may be intercepted by structural resonances. After characterizing the improved Gabor expansion coefficients in an rev/minF spectrum, Fig. 13(b), three main order components (orders 11.1, 36, and 144) can be found. They correspond to the revolution of the CVT driven-sheave, and the meshing frequencies of spur gears G22–G31, and helical gears G11–G21, respectively. Fig. 14 illustrates the masked

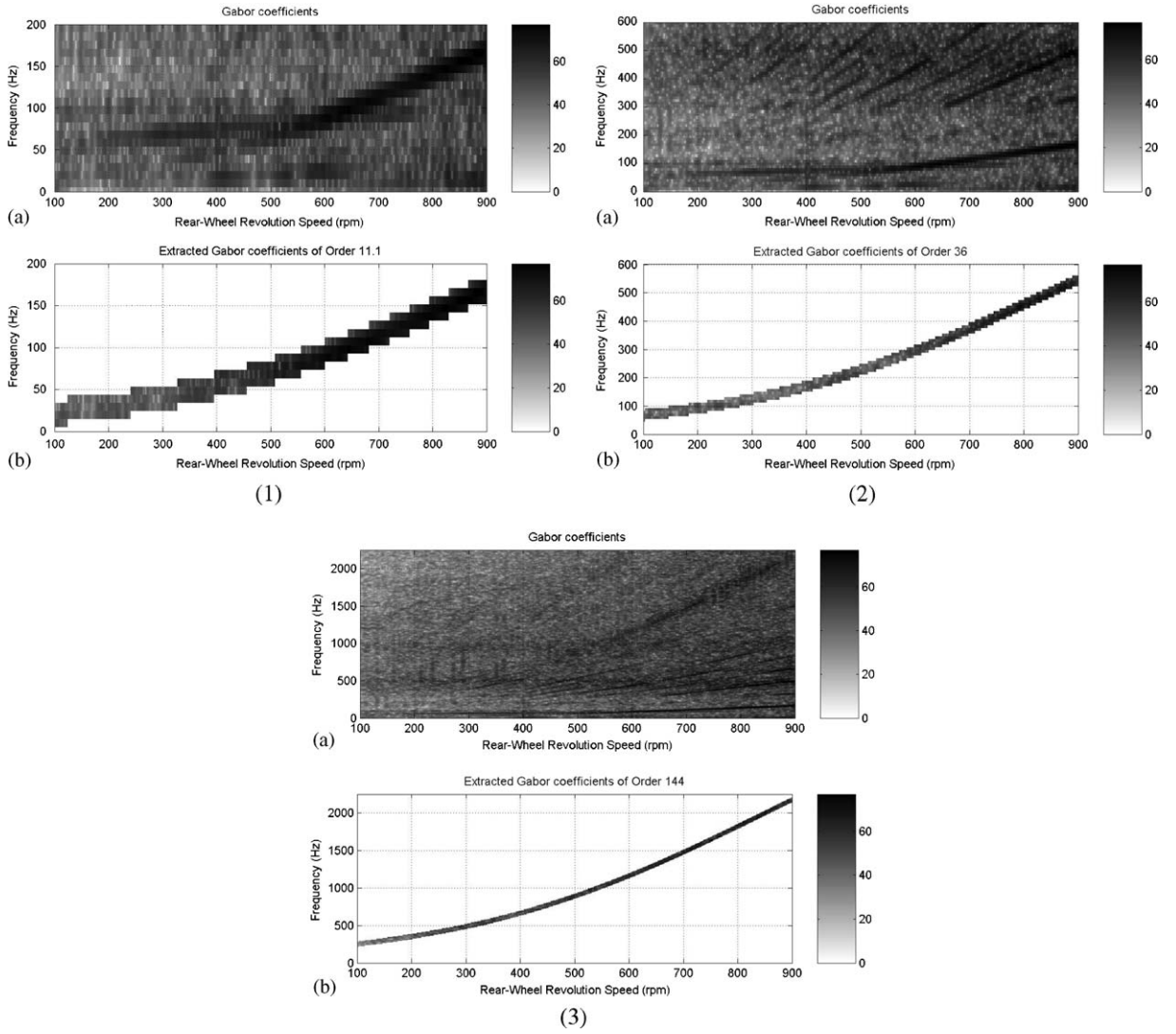

Fig. 14. Local rev/min-spectrum of Gabor expansion coefficients for (1) order-11.1, (2) order-36, and (3) order-144, where (a) the local rev/min-spectra of Gabor coefficients and (b) masked Gabor coefficients.

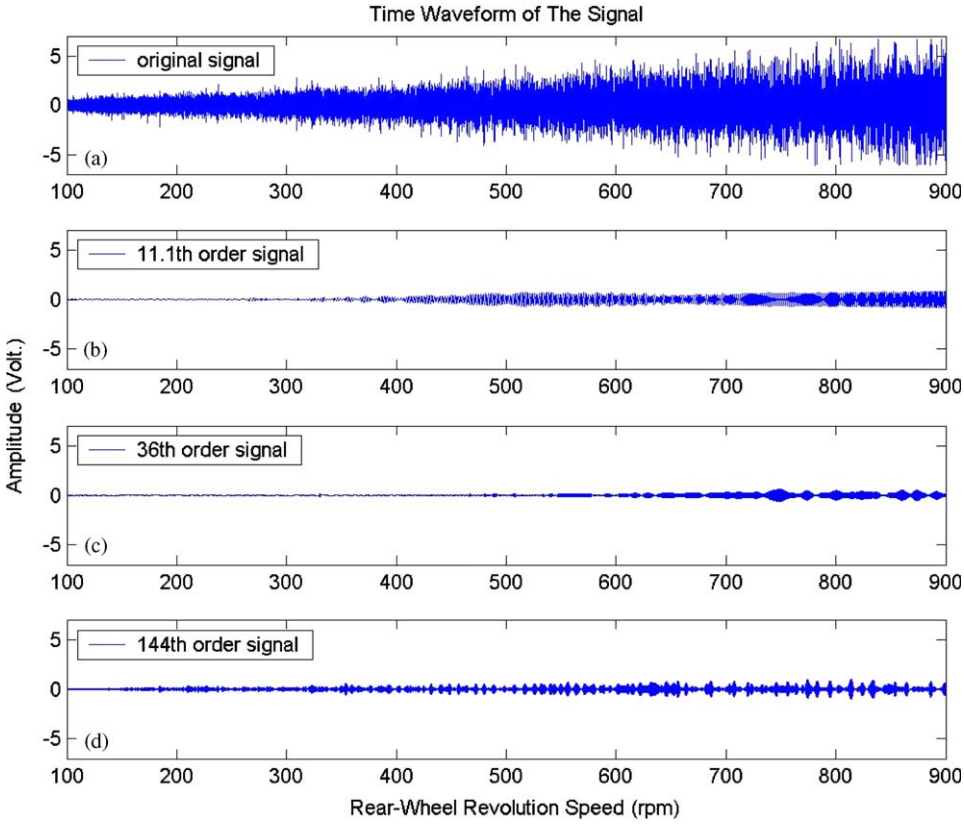

Fig. 15. Time waveforms of vehicle-B riding noise along rear-wheel speed: (a) original measured noise, (b) extracted CVT-driven-pulley noise (order-11.1), (c) extracted helical-gear meshing noise (order-144), and (d) extracted spur-gear meshing noise (order-36).

coefficients for these three orders. Time histories of three specific order components are subsequently computed by using the Gabor expansion function. Fig. 15 illustrates the original acquired signal and three tracked order components. This process helps assess contributions of individual orders on overall riding noise. The sound pressure levels (SPL) along rear-wheel speed are computed and plotted in Fig. 16. As the noise levels are ranked, the outcome can be applied for further noise reduction. Some interesting observations are summarized below.

- Order-11.1 component arising from the CVT driven pulley dominates the noise level, especially as the rear-wheel speeds up to 400 rev/min, equivalent to a vehicle speed of 30 km/h.
- The component of order-144 helical-gear noise secondly contributes to the overall SPL. Around the rear-wheel speed of 650 rev/min, equivalent to a vehicle speed of 45 km/h, the helical-gear noise is comparable to CVT driven-pulley noise.

4. Concluding remarks

The paper addresses the investigation on an improved Gabor OT technique to especially handle order/spectral crossing problems that have not drawn researchers' attention yet. Based on the idea from engineering observation, the edge detection and removal of order/spectral crossing regions, and the averaging of Gabor coefficients are proposed to improve mask operation as well as to obtain modified coefficients for reconstructing target orders. A synthetic signal with a crossing-order event is designated to compare the

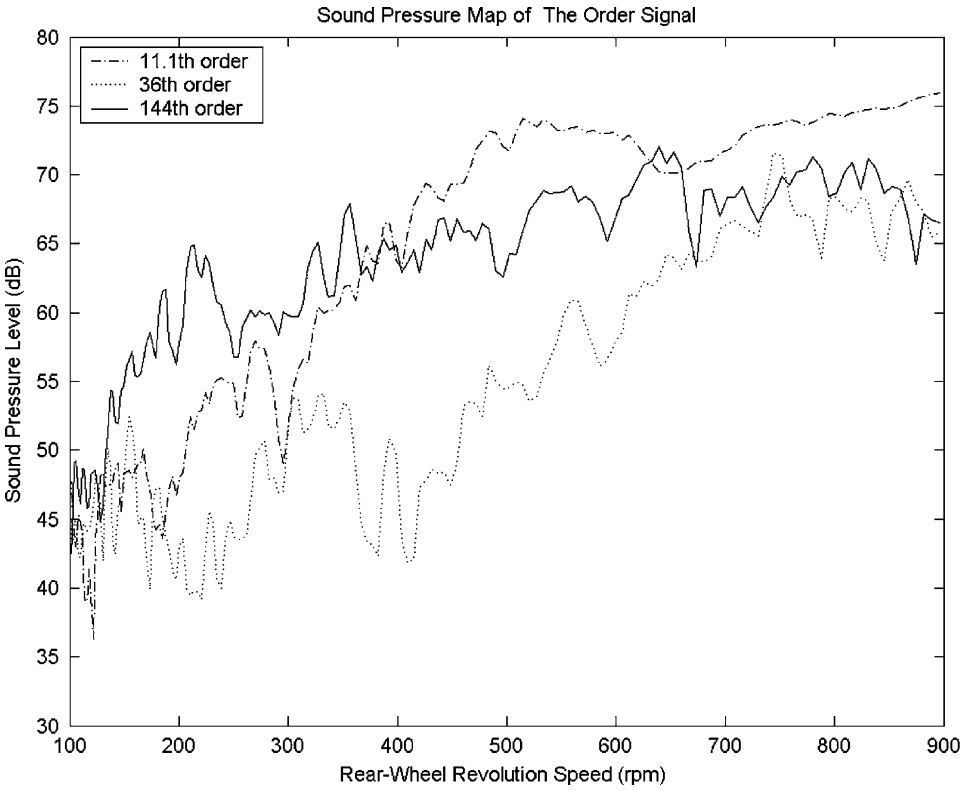

Fig. 16. SPL of characteristic order components along rear-wheel speed (order-11.1 belt noise; order-36 spur-gear meshing noise; order-144 helical-gear meshing noise).

performance for the original and improved schemes. Additionally, two practical works are conducted to justify its effectiveness in engineering applications.

Acknowledgments

This work was supported by the National Science Council of Republic of China under Grant NSC-91-2212-E-008-011. This funding is gratefully acknowledged.

References

[1] R. Potter, A new order tracking method for rotating machinery, *Sound and Vibration* 24 (9) (1990) 30–34.
[2] Sh. Qian, Gabor expansion for order tracking, *Sound and Vibration* 37 (6) (2003) 18–22.
[3] M.-Ch. Pan, J.-X. Chen, Transmission noise identification using two-dimensional dynamic signal analysis, *Journal of Sound and Vibration* (262) (2003) 117–140.
[4] H. Vold, J. Leuridan, High resolution order tracking at extreme slow rates, using kalman tracking filter, SAE Paper 931288, 1993.
[5] H. Vold, M. Mains, J. Blough, Theoretical foundations for high performance order tracking with the Vold–Kalman Tracking Filter, SAE Paper 972007, 1997.
[6] M.-Ch. Pan, Y.-F. Lin, Further exploration of Vold–Kalman-filtering order tracking with shaft-speed information—I: theoretical part, numerical implementation and parameter investigations, *Mechanical Systems and Signal Processing* 20 (5) (2006) 1134–1154.
[7] M.F. Albright, Sh. Qian, A comparison of the newly proposed Gabor order tracking technique vs. other order tracking methods, SAE Paper No. 2001-01-1471, 2001.
[8] M.-Ch. Pan, Z.-W. Liao, Biomedical signal reconstruction using Gabor spectral tracking technique, *International Journal of Information Acquisition* 3 (1) (2006).
[9] D. Gabor, Theory of communication, *Journal of the IEE* 93 (3) (1946) 429–457.
[10] M.J. Bastiaans, Gabor's expansion of a signal into Gaussian elementary signals, *Proceedings of the IEEE* 68 (1980) 538–539.

[11] M.J. Bastiaans, A sampling theorem for the complex spectrogram, and Gabor's expansion of a signal in Gaussian elementary signals, *Optical Engineering* 20 (4) (1981) 594–598.
[12] L. Auslander, I.C. Gertner, The discrete Zak transform application to time–frequency analysis and synthesis of nonstationary signals, *IEEE Transactions on Signal Processing* 39 (4) (1991) 825–835.
[13] M. Zibulski, Y. Zeevi, Oversampling in Gabor scheme, *IEEE Transactions on Signal Processing* 41 (1993) 2679–2683.
[14] Sh. Qian, D. Chen, Discrete Gabor transform, *IEEE Transactions on Signal Processing* 41 (7) (1993) 2429–2438.
[15] M. Sonka, V. Hlavac, R. Boyle, *Image Processing, Analysis, and Machine Vision*, second ed., Brooks/Cole Publishing Co., Pacific Grove, CA, 1999.
[16] M.-Ch. Pan, Ch.-Y. Huang, Dynamic signal processing using advanced time–frequency analysis, *Journal of Chinese Engineers* 27 (7) (2004) 1087–1092.